X-622-67-460

NASA TM X- 55954

THE RADIATION BALANCE OF THE EARTH-ATMOSPHERE SYSTEM OVER BOTH POLAR REGIONS OBTAINED FROM RADIATION MEASUREMENTS OF THE NIMBUS II METEOROLOGICAL SATELLITE

EHRHARD RASCHKE
FRITZ MÖLLER
WILLIAM R. BANDEEN

SEPTEMBER 1967

NASA
GODDARD SPACE FLIGHT CENTER
GREENBELT, MARYLAND

X-622-67-460

THE RADIATION BALANCE OF THE EARTH-ATMOSPHERE SYSTEM OVER BOTH POLAR REGIONS OBTAINED FROM RADIATION MEASUREMENTS OF THE NIMBUS II METEOROLOGICAL SATELLITE

by
Ehrhard Raschke*
Laboratory for Atmospheric and Biological Sciences

Fritz Möller
Meteorologisches Institut der Universität München, Germany

William R. Bandeen
Laboratory for Atmospheric and Biological Sciences

September 1967

GODDARD SPACE FLIGHT CENTER
Greenbelt, Maryland

*On leave from the University of Munich, Germany, as a National Academy of Sciences Post-Doctoral Resident Research Associate.

ABSTRACT

Measurements of the outgoing emitted longwave radiation and the reflected solar radiation were obtained for the first time over the entire globe from the Nimbus II meteorological satellite. These data were obtained during the period 16 May - 28 July, 1966 and covered the onset and development of the summer and winter seasons in the Northern and Southern hemispheres, respectively.

Nimbus II carried a five-channel medium resolution radiometer, two channels of which received longwave radiation and reflected solar radiation in wideband spectral intervals from 5.0 to 30.0 microns and 0.2 to 4.0 microns, respectively. From these "filtered beam" measurements the outgoing "unfiltered" radiation fluxes were calculated using empirical integration techniques. The method of Wark et al. [40] was applied in principle to compute the outgoing flux of emitted longwave radiation. The flux of reflected solar radiation was computed, utilizing empirically derived models of the dependence of the reflection properties of the earth-atmosphere system on the zenith angles of the sun and the measured beam and on the relative azimuth between the two.

The results of the outgoing longwave radiation, the albedo, and the radiation balance of the earth-atmosphere system were obtained as averages for five subperiods, each of a half month's length. As an example, results obtained for the period 1-15 July, 1966 over both polar regions are presented and discussed in the form of maps in this paper.

The albedo over the central Arctic north of 80°N diminished continuously from May to the end of July from 68% to 50% due to the melting of ice and snow surfaces. The radiation balance only during the first half of July became slightly positive (+0.012 cal cm^{-2} min^{-1}) there. During all other subperiods, it resulted in a net radiation flux toward space.

Over the Antarctic during this season the radiation balance is almost entirely determined by the outgoing longwave radiation flux.

The global albedo for all five subperiods was found to be about 30%. This value is considerably less than earlier accepted values ranging between 34% and 43%. The radiation balance over the entire globe resulted in a slight energy gain of +0.002 cal cm^{-2} cm^{-1} during the second half of May and a deficit between -0.003 and -0.007 cal cm^{-2} min^{-1} during the other four subperiods.

CONTENTS

ILLUSTRATIONS

ILLUSTRATIONS (con't)

TABLES

THE RADIATION BALANCE OF THE EARTH-ATMOSPHERE SYSTEM OVER BOTH POLAR REGIONS OBTAINED FROM RADIATION MEASUREMENTS OF THE NIMBUS II METEOROLOGICAL SATELLITE

1. INTRODUCTION

The radiation balance of the earth-atmosphere system over each geographic location describes the energy gain or loss of the system resulting from two processes: absorption of incoming solar electromagnetic radiation and emission of longwave thermal radiation. Absorption, reflection and scattering of incident solar radiation and the emission of longwave radiation to space takes place mainly at the surface and in atmospheric layers up to a height of about 50 km. Therefore, the radiation balance determines primarily the net radiation flux at the level of about 50 km, and should be closely related to all atmospheric processes below that level.

Earlier investigations ([2], [10], [11], [20], [28], [36], [39]) showed clearly that in the annual average, energy is gained at low latitudes and lost at high latitudes. This forms a thermal gradient requiring an energy exchange between low and high latitudes by the atmospheric circulation and also by ocean currents. These investigations, however, were based on observations whose reliability was not very satisfactory over both polar regions and over oceanic areas [3]. Moreover, the computations of the fluxes of absorbed and emitted radiation, could take into account only in very simplified models all physical processes taking part in the radiative transfer within the atmosphere and at the ground. Thus widely differing results were obtained.

Radiometric measurements of reflected solar radiation and of emitted thermal radiation from artificial satellites should provide an ideal basis to observe steadily and very accurately the radiation balance on a global scale. Such measurements were carried out beginning with the launching of the first meteorological satellite Explorer VII and continuing with different instruments from several TIROS satellites ([7], [21], [33], [37]). These satellites, however, "observed" the earth no farther poleward than 60°N and 60°S. Nimbus II, launched on May 15, 1966 and the succeeding satellites ESSA 3 and ESSA 5 performed the first radiation measurements over the entire globe. Considerable computational efforts are necessary to determine from the filtered beam measurements of the radiometer the desired quantities, namely the outgoing fluxes of reflected

solar radiation and of longwave thermal radiation, leaving the atmosphere to space.

It is the purpose of this paper to discuss the results of the radiation balance and related quantities, which were obtained from Nimbus II measurements during the period 16 May to 28 July, 1966 over both polar regions. This period was divided into 5 smaller intervals each of a half month's duration, of which one was chosen here (1-15 July, 1966) to demonstrate our calculation methods and the results. All other results and the computation methods in more detail will be described in a final report on this research [32].

2. THE NIMBUS II MEASUREMENTS

The satellite Nimbus II was launched on May 15, 1966 into a sun-synchronous, nearly polar orbit [31]. At a mean height of 1140 km above the earth's surface, it crossed the equator in the northward direction at around local noon and in the southward direction on the opposite side of the earth at around local midnight. Its orbital period of 107 minutes and its height provided that generally each area element on the earth was observed at least once in the daytime and once in the nighttime within a 24 hr interval. But difficulties in the data acquisition at orbit did not allow the recording of all data, thus causing gaps in the observational coverage of the globe.

A scanning five-channel medium resolution radiometer aboard Nimbus II measured the reflected solar radiation in the spectral range from 0.2 - 4.0 microns and the emitted thermal radiation in the spectral range from 5.0 to 30.0 microns. In a third channel infrared radiation between 10 and 11 microns, a measure of the temperature of the underlying surface (clouds and/or ground), was received. The instantaneous angular field of view of the radiometer of about 2.5 degrees enabled a spatial resolution on the earth's surface from about 50 km (at the subsatellite point) to about 110 km (at a nadir angle of 40 degrees). A calibration source aboard Nimbus II provided for correcting the measurements of infrared radiation for changes in the instrumental response. The measurements of reflected solar radiation were checked by comparison of all measurements obtained over cloudless portions of the Sahara. No changes in the instrumental response could be observed in these measurements.

3. METHOD OF COMPUTATION

The net radiation flux or radiation balance Q at a surface element, whose geographic coordinates on the earth's surface are λ and ϕ is defined as the

algebraic sum of all radiation fluxes crossing it:

$$Q(\lambda, \phi, d) = S(\lambda, \phi, d) - R(\lambda, \phi, d) - E(\lambda, \phi, d) \quad . \tag{1}$$

In Equation (1) S, R and E are the fluxes of incoming and reflected solar radiation and of emitted longwave radiation, respectively. The letter d designates that day, for which Equation (1) applies. The reference area is assumed to be perpendicular to the earth's radius vector passing through it.

The fluxes R and E outgoing from an observed element on the earth's surface have been computed by integrating the radiance N over the hemisphere above that surface:

$$\text{Flux} = \int_0^{2\pi} \int_0^{\pi/2} N(\theta, \psi) \sin\theta \cos\theta \, d\theta \, d\psi \quad . \tag{2}$$

In this general equation θ and ψ are the zenith angle and the relative azimuth angle (with respect to the vector of incident solar radiation) of a measurement by the Nimbus II radiometer.

The computational procedure presumes the geometric generalization that the atmosphere and surface of the earth form the surface of an imaginary sphere, having the mean radius of the earth (6371 km), but still having the same physical properties as the actual earth-atmosphere system. The computational procedures of both outgoing radiation fluxes required further generalized assumptions to convert the measured "filtered" radiances into the "unfiltered" radiances and to perform the integration over the upward hemisphere. According to the method of Wark et. al. [40] the unfiltered radiance of longwave thermal radiation was computed from the measured "filtered" radiance using a relation, which was found from calculated values of the outgoing radiance from a large set of atmospheric profiles [26].

Figure 1 shows as dots calculated radiances in the vertical direction. Encircled points mark results computed for a zenith angle $\theta = 78.5°$. These results show a nearly linear relation between the "filtered" and "unfiltered" radiances due to the wide filter range (5.0 - 30.0 microns) of the channel used for the measurements. A relation which describes the dependence of N on the zenith angle was determined statistically by Lienesch and Wark [27] from radiation data of TIROS satellites. An assumption of symmetry of emitted longwave radiation with respect to the azimuth angle ψ was made in this study.

The thermal radiation outgoing from an area is strongly correlated with the temperature of the underlying surface [30]; thus it is largely dependent on daily changes of the cloudiness and on the temperature at the ground. Over most regions of the earth Nimbus II measured longwave radiation twice a day, close to local midnight and local noon. It has been assumed that these measured values are mean values for nighttime and daytime conditions, respectively. The daily mean of the flux then was calculated by weighting each of both values according to the duration of the daytime and nighttime periods, respectively.

The calculation of the reflected flux of solar radiation during a day from an "observed area" is more complicated, since the reflection properties of the earth-atmosphere system show clearly a strong dependence on both the zenith and azimuthal angles (θ and ψ) of the measurements and on the sun's elevation above the horizon (e.g. [5], [8], [12], [18]). This required, as mentioned above, the determination of the solar radiation reflected into the upward hemisphere from the measured beam radiance N and an extrapolation from the moment of measurement to the interval from sunrise to sunset over the same area. The simplifying assumption of a Lambertian surface, as was done in the past by several authors ([7], [29], [33], [41]) probably caused an underestimation of the reflection properties of the earth-atmosphere system, especially at very low solar elevation angles.

The method of calculating the flux of reflected solar radiation between sunrise and sunset is only briefly outlined here. From the measured "filtered" radiance N_f the bidirectional reflectance ρ_f' is obtained by means of Equation (3):

$$\rho_f'(\theta, \psi, \zeta') = \frac{N_f(\theta, \psi)}{S_f(d) \cos \zeta'} \left[sr^{-1}\right] \tag{3}$$

Here ζ' is the solar zenith angle at the moment of measurement. The "filtered" irradiance S_f of incoming solar radiation is obtained by integrating the product of the extraterrestrial spectral irradiance of solar radiation [23] and the filter function of the instrument over all wavelengths. Because of the wide range (0.2 - 4.0 micron) of that filter it was assumed that ρ_f' in Equation (3), which refers to the "filtered" radiation only, is equal to the mean reflectance ρ' over the entire spectrum.

To determine the ratio r between the radiation reflected into the entire hemisphere and the incident solar irradiance at the zenith angle ζ' an integration is needed over θ and ψ analogous to Equation (2). Therefore diagrams were derived from many measurements of reflected solar radiation ([5], [8], [13],

[35]) showing the ratio $X = r/\rho$ (where $\rho = \pi \cdot \rho'$) versus θ and ψ. One of these diagrams, which were drawn for only three ranges of the sun's zenith angle ζ' (viz., 0° - 35°, 35° - 60°, 60° - 80°), is shown in Figure 2. It demonstrates that at low sun ($60° \leq \zeta' \leq 80°$) the ratio r/ρ is very small for small ψ but large θ, corresponding to a bright horizon in the direction of the sun and also a relative high radiance of backscattered radiation for values of ψ near 180°. The reflectance $\rho = \pi \cdot \rho'$ is small in the nadir and larger towards all points of the horizon. The integral of r/ρ over the hemisphere is π. The ratio r, often called the directional reflectance [8] is still a function of the sun's zenith angle. Thus for the computation of the outgoing flux of solar radiation reflected to space from an area between sunrise and sunset, a statistical relation, obtained from the above mentioned measurements, was used. In Figure 3 this relation is compared with results recently obtained statistically by several authors from TIROS measurements.

In a further step the mean daily albedo, which is the ratio between daily reflected and daily incident solar radiation, was obtained from a single measurement of r by integrating over all solar elevations during the day from sunrise to sunset. With a simple model (Table IX in [9]) a mean refraction of solar radiation in the atmosphere was taken into account in calculations of both the incoming and the reflected flux of solar radiation. The solar constant S_0 was assumed to be 2.0 cal cm^{-2} min^{-1} although recently Drummond et al. [14] found from airplane measurements a lower value of 1.95 cal cm^{-2} min^{-1}.

All single results were averaged within grid fields of the size of 5 degrees of longitude and 2 to 5 degrees of latitude. Measurements in both spectral ranges obtained at zenith angles larger than 45 degrees were omitted to avoid excessive limb effects in the results. The albedo of an observed area was then defined to be the ratio of R over S. The difference between S and R simply describes the absorbed amount of solar radiation.

These simplified models, indeed, may cause considerable errors in the results if used for specific geographic areas and meteorological conditions such as cloudless, partially cloudy, and overcast cases. In investigations of the radiation balance over smaller geographic locations more sophisticated models should be used. These however have not been derived so far, due to the lack of observational data. It is believed, however, that such errors are averaged out in these investigations on a global scale.

4. RADIATION BALANCE OVER THE ARCTIC BASIN

During that time when data of the Nimbus II medium resolution radiometer were available the sun's declination ranged between +19 and +23 degrees. Thus,

the earth-atmosphere system over the North-Pole received during a 24 hour interval even more solar radiation than regions in the northern subtropics. But ice and snow surfaces and a mean cloud coverage of 6/10 to 10/10* caused more than 50% of the incoming radiation to be reflected back to space. Figure 4 illustrates this for the period 1-15 July, 1966.

In Figure 4 the 50% isoline follows (except south of Greenland) closely the climatological boundary of a mean ice coverage of 0.8-1.0 of the arctic ocean during this period [38]. The same position of that boundary is confirmed by the Nimbus II AVCS photographs of the same period. The albedo over the Norwegian Sea and over the Barents Sea, which were icefree but also covered with 6/10 to 10/10 of clouds, is remarkably less than over the aforementioned areas, demonstrating the high influence of the reflectance of the ice surface on the total albedo and, therefore, also on the radiation budget of the earth-atmosphere system. Since the ocean water has a reflectance of less than 10% the albedo of the cloud-ocean surface system is strongly diminished even over dense cloud covers. The reflectance of the ground contributes much to the amount of shortwave radiation flux emerging from the upper surface of the clouds.

The albedo over Greenland sharply rises from the coastline to the interior from 60% to more than 80%. This corresponds to the surface albedoes of 71% to 79% measured by Kasten [24] over the Greenland ice cap. The albedo as measured from space over Greenland remains nearly constant (from May to July), while the average albedo of the northern hemisphere (as shown in Table I) decreases due to melting of ice and snow surfaces. This decrease of the albedo and the very high sun during the end of June and the first half of July causes the amount of absorbed solar radiation to exceed the radiation loss by outgoing longwave radiation over the pole during the first half of July.

Figure 5 shows the field of outgoing longwave radiation for the same period. Due to a cloud cover with mostly stratocumulus, altostratus, and stratus this field is nearly uniform. Only over the high inland ice of Greenland and over the thick ice mantle on the East Siberian Sea areas of lower emission occur. As Table I shows the outgoing longwave radiation increases only slowly during the beginning of the northern summer until June, then remains constant during July (period 4 and 5). This holds also for the mean temperature of the earth-atmosphere system. Thus changes in the amount of the incoming solar radiation

*Maps of the mean cloud coverage over the Northern hemisphere were obtained for the same periods of Nimbus II measurements through the courtesy of the USAF Environmental Technical Applications Center, Washington, D.C. One of them is shown in Figure 4a, in this report.

Table I

Zonal averages of the incoming (S) and absorbed (S - R) solar radiation, the emitted longwave radiation (E), the radiation balance (Q) and the albedo (R/S) over the northern hemisphere. Periods 1 - 5 are listed in Table II.

Latitude	Period	R/S %	S	S - R	E	Q
			All in cal cm^{-2} min^{-1}			
85°N	1	66.3	0.682	0.230	0.284	-0.054
	2	65.7	0.746	0.256	0.296	-0.040
	3	61.9	0.762	0.290	0.312	-0.012
	4	56.6	0.738	0.320	0.308	+0.012
	5	55.2	0.670	0.300	0.310	-0.010
80°N	1	68.9	0.675	0.210	0.282	-0.072
	2	67.9	0.736	0.236	0.296	-0.060
	3	61.6	0.756	0.290	0.310	-0.020
	4	57.7	0.728	0.308	0.309	-0.001
	5	56.1	0.660	0.290	0.312	-0.022
75°N	1	67.7	0.662	0.214	0.286	-0.072
	2	64.6	0.724	0.256	0.300	-0.044
	3	58.9	0.740	0.304	0.306	-0.002
	4	55.8	0.715	0.316	0.310	+0.006
	5	48.8	0.648	0.332	0.310	+0.022
70°N	1	60.3	0.650	0.258	0.296	-0.038
	2	52.3	0.705	0.336	0.312	+0.024
	3	47.2	0.720	0.380	0.315	+0.065
	4	45.7	0.696	0.378	0.320	+0.058
	5	44.9	0.635	0.350	0.315	+0.045
65°N	1	47.8	0.644	0.336	0.305	+0.031
	2	39.9	0.690	0.415	0.327	+0.088
	3	39.3	0.700	0.425	0.322	+0.103
	4	41.1	0.680	0.400	0.327	+0.073
	5	40.7	0.632	0.375	0.327	+0.048

as well as changes in the albedo during this time of the year solely influence the radiation balance of the Arctic.

Figures 6 and 7 show maps of the radiation balance (i.e., the net radiation flux at the top of the atmosphere) for two periods. During the second half of

May (Figure 6) the radiation balance north of 70°N is everywhere negative except over the Norwegian Sea, where lower albedoes occur over the icefree sea surface. Here clearly the influence of the polar ice cap on the radiation budget is demonstrated. This subject has been discussed by several authors ([16], [39]). Maxima of the deficit occur over Greenland and over the East Siberian Sea. They remain deficit areas even during the first half of July, when over all other areas the amount ot absorbed solar radiation slightly exceeds the emitted radiation (Figure 7). Zonal averages in Table I show that the radiation balance becomes negative towards the end of July north of 75°N due to decreasing elevation of the sun above the horizon. These results do not agree with studies of other authors. Vowinkel and Orvig [39] found positive values for the radiation balance over the central arctic in their very detailed analyses only for June, while Fletcher (Figure 10 in [16]) has obtained a positive balance also for the months May and July. Vowinkel and Orvig [39], perhaps might have underestimated the cloud cover in upper layers of the atmosphere [19].

5. RADIATION BALANCE OVER THE ANTARCTIC

The Antarctic continent south of 71°S did not receive any solar radiation from May to July. Thus the radiation balance during this period consists entirely of the loss of radiative energy by emission of thermal radiation. Figures 8 and 9 show the fields of outgoing longwave radiation and of the equivalent blackbody temperature of infrared radiation between 10 and 11 microns, which is very close to the temperature of the underlying surface. The pattern of both fields over the southern oceanic areas is almost zonal. The 250°K isotherm in Figure 9 closely follows the mean climatological pack ice boundary during July [38]. Over the continent the isolines follow more or less the geographic contours. At the Soviet Plateau close to Queen Maud Land, with elevations of more than 3500 meters above sea level, surface temperatures of less than 210°K (see also Figure 77 in [6]) cause a minimum in the field of outgoing longwave radiation. High cloud surfaces over the west coast of South America and east of the Antarctic Peninsula are clearly associated with areas of low temperature in Figure 9 and therefore with lower emitting areas in Figure 8.

Solar radiation is available only north of 71°S to compensate for the loss of radiative energy. Because of the minimum of longwave emission in the central Antarctic continent and of the increase of emission toward lower latitudes the radiation balance shows a maximum radiation deficit of more than 0.24 cal. cm^{-2} min^{-1} in a zonal ring between 55° and 70°S during May (Figure 10). This ring expands slightly during the first half of June, but becomes smaller toward July (Figure 11) due to decreasing temperatures by radiative cooling and the equatorward expansion of the pack ice at its southern

boundary and an increase of incoming solar radiation at its northern boundary.

Zonal averages of the radiation balance for all five periods (Table II) show clearly a rapid cooling of the inner Antarctic from May to the end of June with a reduced rate during July. At 70° - 80°S the cooling is nearly compensated for in July by advection. At lower latitudes the maximum of the radiation deficit occurs at the end of June at lowest elevations of the sun above the horizon.

Gabites' (in [15]) and Simpson's [36] results on the radiation balance of the earth-atmosphere system are added for comparison in Table II. Gabites, who used observational material from the IGY (1957-1958), obtained the closest agreement with our results at 60°S and 65°S. Simpson's values over the Antarctic continent show a radiation loss which is too high, since he derived the temperatures there by extrapolation from lower latitudes.

Table II

Zonal averages of the radiation balance over the southern hemisphere. Values in cal cm^{-2} min^{-1}.

	Period	85°S	80°S	75°S	70°S	65°S	60°S	55°S
Nimbus II	16-31 May	-0.190	-0.194	-0.208	-0.238	-0.250	-0.248	-0.234
	1-15 June	-0.185	-0.195	-0.204	-0.233	-0.250	-0.256	-0.245
	16-30 June	-0.180	-0.185	-0.195	-0.228	-0.252	-0.256	-0.250
	1-15 July	-0.176	-0.183	-0.193	-0.222	-0.240	-0.245	-0.238
	16-28 July	-0.170	-0.183	-0.193	-0.218	-0.238	-0.240	-0.225
Gabites (in [15])	June	-0.186	-0.200	-0.225	-0.240	-0.250	-0.247	-0.233
	July	-0.180	-0.195	-0.225	-0.235	-0.250	-0.243	-0.230
Simpson [36]	June	-0.253		-0.254		-0.245		-0.226
	July	-0.253		-0.253		-0.240		-0.213

6. GLOBAL RADIATION BALANCE

The geographic distribution of the radiation balance during the first half of July over the entire globe is shown in Figure 12. During this time an energy surplus of absorbed solar radiation over emitted longwave radiation is found nearly everywhere north of 10°S. Maxima of energy gain occur over the

relatively cloudless northern subtropical oceans. The large desert areas of North Africa and Arabia in contrast show a deficit, which has been predicted by Budyko [11] for the annual average. This deficit is caused by the high values of the albedo (30% to 40%) and by the high surface temperature of those areas. Over the entire southern hemisphere south of 10°S the radiation balance everywhere is negative. The deficit over land was found to be somewhat higher than over the surrounding oceanic areas at the same latitude.

The numerical values in Figure 12 clearly differ from the figures obtained by Möller [29] in a preliminary study, mainly due to the fact that the careful corrections we have developed in section 3 were not applied in his investigations of Nimbus II measurements during the same period.

Table III summarizes the global averages, of the albedo, of the absorbed solar radiation, of the emitted longwave radiation, and of the radiation balance. These values in contrast to the zonal averages shown in Tables I and II show no significant changes with time indicating that the entire globe changes its radiation budget, if at all, only over a longer period than that of these satellite measurements. The global albedo was found to be only 29 - 30% which is considerably less than all values between 34% and 43% obtained by several authors in earlier studies ([1], [4], [10], [17], [36]). The global average of the radiation balance was slightly positive at the end of May, and ranged between -0.003 cal cm^{-2} min^{-1} and -0.007 cal cm^{-2} min^{-1} during all other periods. This slight radiation deficit was earlier suggested by Simpson [36] for the same season. But due to uncertainties in our computational methods as well as due to the uncertainties in the true value of the solar constant, these values do not allow definite conclusions about the heat budget of the earth-atmosphere system. They indicate, however, that a revision of the hitherto-given models of the budget of solar and terrestrial radiation appears necessary. Unfortunately, the period of available radiation measurements from the Nimbus II satellite was too short to correlate our results on the radiation balance with indices describing typical features of the circulation [22].

Table III

Global Radiation Balance from Nimbus II Measurements

	Albedo %	Absorbed Solar Radiation cal cm^{-2} min^{-1}	Outgoing Longwave Radiation cal cm^{-2} min^{-1}	Radiation Balance cal cm^{-2} min^{-1}
May 16-31	30.1	0.341	0.339	+0.002
June 1-15	30.6	0.337	0.342	-0.005
June 16-30	30.1	0.338	0.345	-0.007
July 1-15	29.1	0.343	0.346	-0.003
July 16-28	29.5	0.342	0.345	-0.003

ACKNOWLEDGMENTS

The authors should like to express their appreciation to Mr. Robert Hite and Mr. Hugh Powell for their extensive efforts in the computer processing of the vast amount of satellite radiation measurements utilized in this study.

REFERENCES

1. Aldrich, L. B., 1919: The Reflecting Power of Clouds. Smithsonian Miscellaneous Collections, 69, No. 10.

2. Alt, E., 1929: Der Stand des Meteorologischen Strahlungsproblems. Meteor. Zeitschrift, 46, 504-513.

3. Ångström, A., 1925: The Albedo of Various Surfaces of Ground. Geografiska Annaler, 6, 323-342.

4. Ångström, A., 1962: Atmospheric Turbidity, Global Illumination and Planetary Albedo of the Earth. Tellus, 14, 435-450.

5. Arking, A., 1965: The Angular Distribution of Scattered Solar Radiation and the Earth Albedo as Observed from TIROS. Institute for Space Studies, New York, Research Reports, July 1, 1964 - June 30, 1965, 47-67.

6. Atlas of the Antarctic (ATLAS ANTARKTIKI), 1966: Moscow-Leningrad, 1966.

7. Bandeen, W. R., M. Halev, and I. Strange, 1965: A Radiation Climatology in the Visible and Infrared from the TIROS Meteorological Satellites. NASA Technical Note D-2534, 30 pp.

8. Bartman, F. L., 1967: The Reflectance and Scattering of Solar Radiation by the Earth. Technical Report, 257 pp, University of Michigan, Contr. NASr-54(03).

9. Baur, F., ed.: Linke's Taschenbuch der Meteorologie, z. Ausgabe, Vol. II. Leipzig, 1953.

10. Baur, F. and H. Philipps: Der Wärmehaushalt der Lufthülle der Nordhalbkugel in Januar und Juli and zur Zeit der Äquinoktien und Solstitien. 1934, 1937 Gerl. Beitr. Geophys., 42, 160-207; 45, 82-132.

11. Budyko, M. I., ed., 1963: Atlas of the Heat Balance of the Earth (Atlas Teplovogo Balansa Zemnogo Shara), Moscow.

12. Coulson, K. L., 1959: Characteristics of the Radiation Emerging from the Top of a Rayleigh Atmosphere. Planet, Space Sci., 1, 265-284.

13. Cherrix, T., and B. Sparkman, 1965: A Preliminary Report on Bidirectional Reflectances of Stratocumulus Clouds Measured with Airborne Medium Resolution Radiometer. NASA X-622-76-48, Goddard Space Flight Center.

14. Drummond, A. J., J. R. Hickey, W. J. Scholes, and E. G. Laue: Multichannel Radiometer Measurement of Solar Irradiance, 1967. The Eppley Laboratory Inc., Reprint Series No. 33, Paper presented at the AIAA Meeting, Jan. 23-26, 67, in New York.

15. Dwyer, L. J., ed., 1960: Antarctic Meteorology — Proceedings of the Symposium held in Melbourne, Febr. 1959, Pergamon Press.

16. Fletcher, J. O., 1965: The Heat Budget of the Arctic Basin and Its Relation to Climate. The RAND Corporation, R-444-PR.

17. Fritz, S., 1949: The Albedo of the Planet Earth and of Clouds. Journ. Meteor., 6, 277-282.

18. Heger, K., 1966: Die von der getrübten Atmosphäre nach aussen gestreute Strahlung. Beitr. z. Physik d. Atm., 39, 12-36.

19. Henderson, P., 1967: Cloud Conditions over the Beaufort Sea. Publ. in Meteorology, No. 86, Dept. of Meteor., McGill University, Montreal, Canada.

20. Houghton, H. G., 1954: On the Annual Heat Balance of the Northern Hemisphere. Journ. Meteor. 11, 3-9.

21. House, F. B., 1965: The Radiation Balance of the Earth from a Satellite Ph.D. Thesis, Dept. of Meteor., The University of Wisconsin.

22. Huschke, R. E., J. O. Fletcher, and R. R. Rapp: An Apparent Statistical Relationship Between Polar Heat Budget and Zonal Circulation. Contr. No. NASr-21-(07), January 1967, RM-5234-NASA, RAND Corporation, Santa Monica, Calif.

23. Johnson, F. S., 1954: The Solar Constant. Journ. Meteor., 11, 431-439.

24. Kasten F., 1963: Meteorologisch-Optische Untersuchungen auf dem grönländischen Inlandeis. Polarforsch, 5, 202-207.

25. Levine, J. S., 1967: The Planetary Albedo Based on Satellite Measurements Taking into Account the Anisotropic Nature of the Reflected and Backscattered Solar Radiation. Masters Thesis, Graduate School of Arts and Sciences, New York University, New York, N.Y.

26. Lienesch, J. H., 1966: private communication.

27. Lienesch, J. H., and D. Q. Wark, 1967: Infrared Limb Darkening of the Earth from Statistical Analyses of TIROS data. Journ. Appl. Meteor., 6, 674-682.

28. London, J., 1957: A Study of the Atmospheric Heat Balance. Final Report, Contract AF 19(122)-165, Research Division, College of Engineering, New York University, New York.

29. Möller, F., 1967: Eine Karte der Strahlungsbilanz des Systems Erde-Atmosphäre für einen 14-tägigen Zeitraum. Meteor. Rundschau, 20, 97-98.

30. Möller, F., and E. Raschke, 1964: Evaluation of TIROS III Radiation Data. NASA Contractor Report - 112 (Grant NsG-305 with University of Munich, Germany).

31. Nordberg, W., A. W. McCulloch, L. L. Foshee, and W. R. Bandeen, 1966: Preliminary Results from Nimbus II. Bull. Am. Meteor. Soc., 47, 857-872.

32. Raschke, E. and M. Pasternak, 1967: The Global Radiation Balance of the Earth-Atmosphere System from Radiation Measurements of the Nimbus 2 Meteorological Satellite. NASA Technical Report (in preparation); see also NASA-X-622-67-383, Aug. 1967.

33. Rasool, S. I., and C. Prabhakara, 1966: Heat Budget of the Southern Hemisphere. Problems in Atmospheric Circulation, ed. by Garcia and Malone, Spartan Books, Wash., D.C., 76-92.

34. Ruff, I., Koffler, R., Fritz, S., Winston, J. S., and Rao, P. K., 1967: Angular Distribution of Solar Radiation Reflected from Clouds as Determined from TIROS IV Radiometer Measurements. ESSA Technical Report, NESC - 38, Washington, D.C.

35. Salomonson, V., 1966: Anisotropy of Reflected Solar Radiation from Various Surfaces as Measured with an Aircraft-Mounted Radiometer. Research Report, Contract NASr-147, Colorado State University, 29 pp.

36. Simpson, G. C., 1928: The Distribution of Terrestrial Radiation. Memoirs of the Royal Meteor. Soc., 3, No. 23.

37. Suomi, V. E., 1961: The Thermal Radiation Balance Experiment on board Explorer VII, NASA Technical Note D-608.

38. U.S. Navy Hydrographic Office: Oceanographic Atlas of the Polar Seas. Part I: Antarctic, 1957, Part II: Arctic, 1958. Washington, D. C., H.O. Pub. No. 705.

39. Vowinkel, E., and S. Orvig, 1964: Radiation Balance of the Troposphere and of the Earth-Atmosphere System in the Arctic. Sci. Rep. No. 9; Contract AF 19(604)-7415, Dept. of Meteor., Montreal.

40. Wark, D. Q., G. Yamamoto, and J. H. Lienesch, 1962: Methods of Estimating Infrared Flux and Surface Temperature from Meteorological Satellites. Journ. Atm. Sci., 19, 369-384.

41. Winston, J. S., 1967: Planetary Scale Characteristics of Monthly Mean Long-Wave Radiation and Albedo and Some Year-to-Year Variations. Monthly Wea. Rev., 95, 235-256.

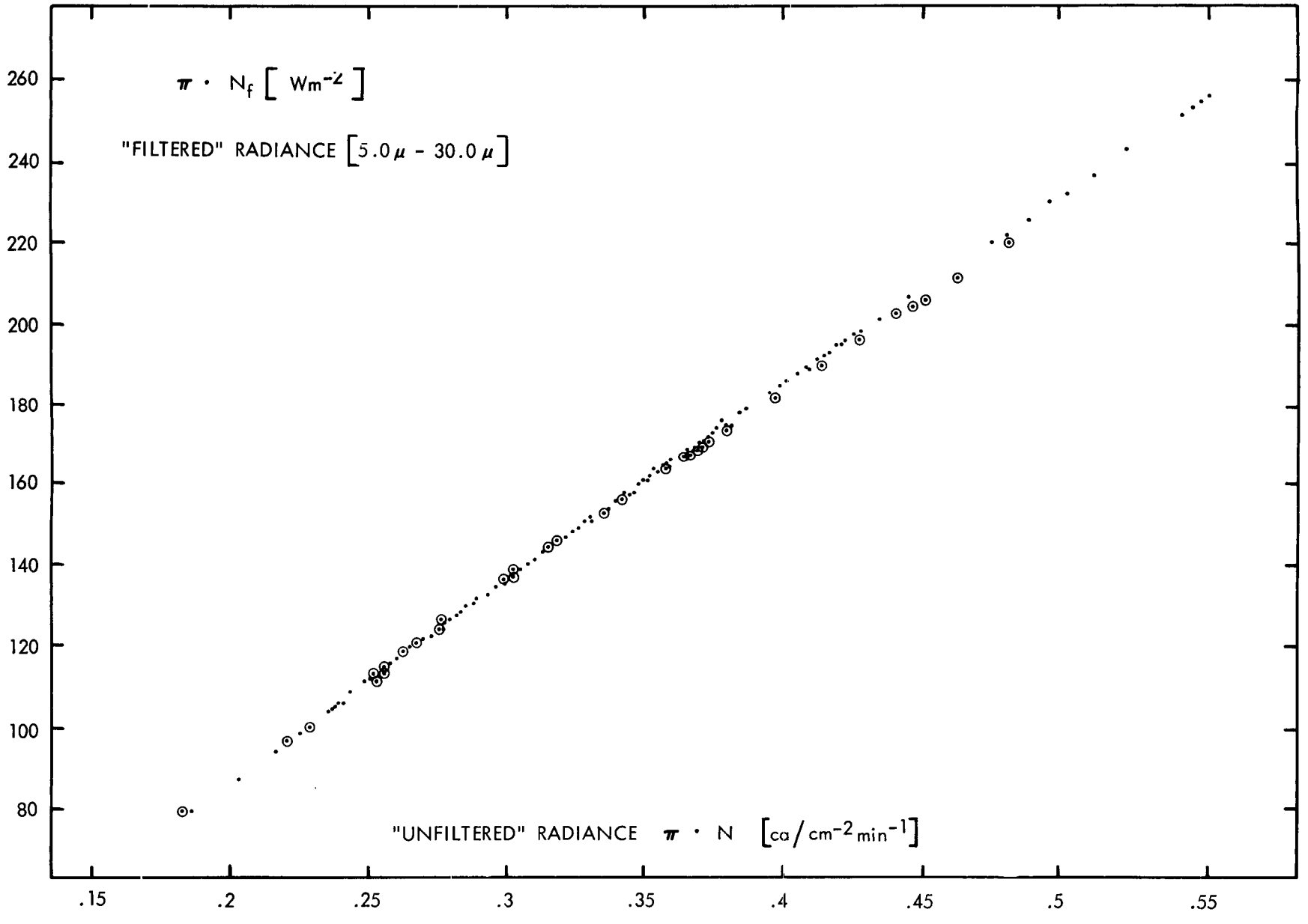

Figure 1. Nimbus II: Relation between the "filtered" (5.0 - 30.0 microns) and "unfiltered" radiance of outgoing longwave radiation

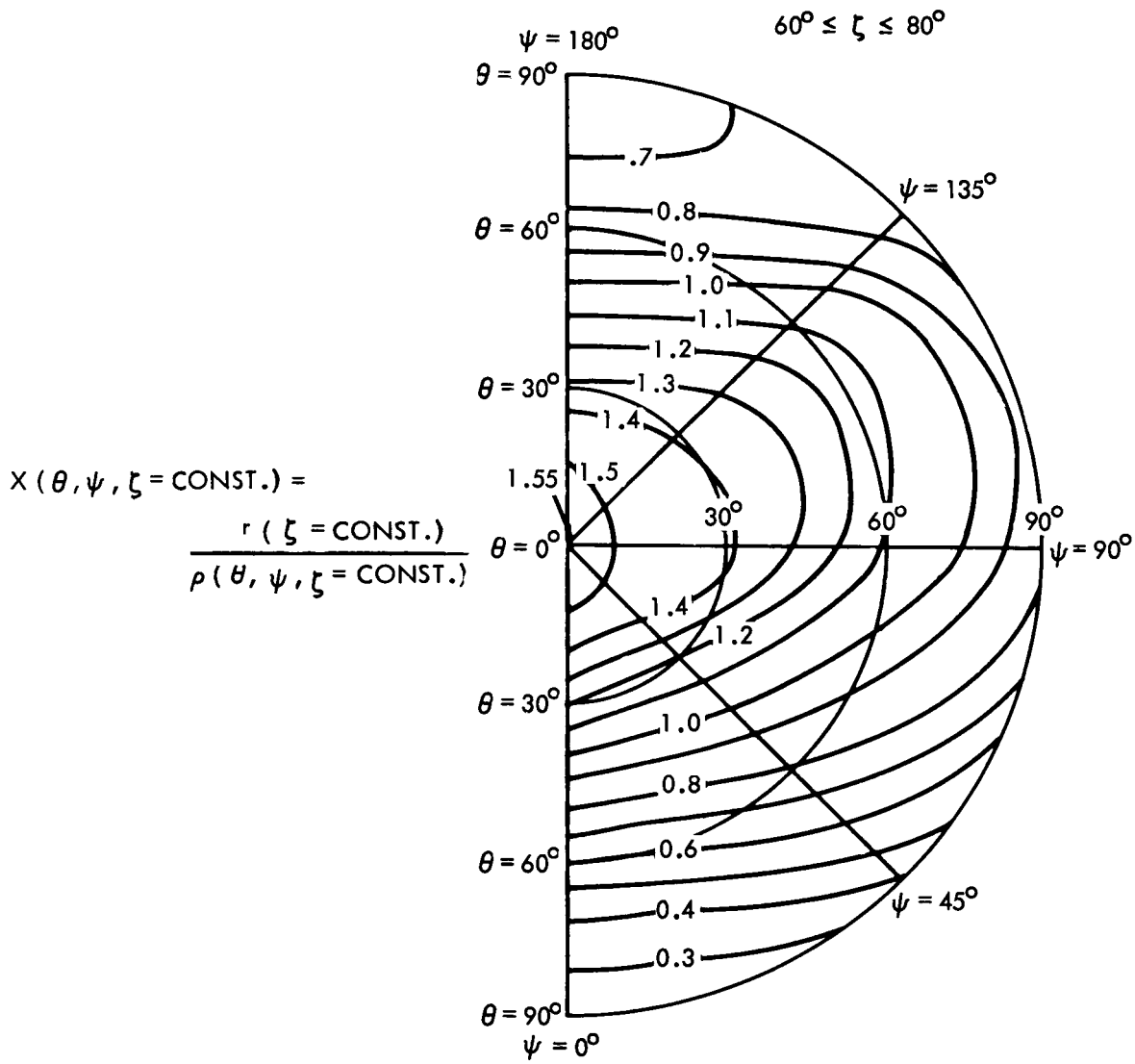

Figure 2. Dependence of the ratio $X = r/\rho$ on the angles θ and x of the measurement at very low sun ($60° \leq \zeta' \leq 80°$)

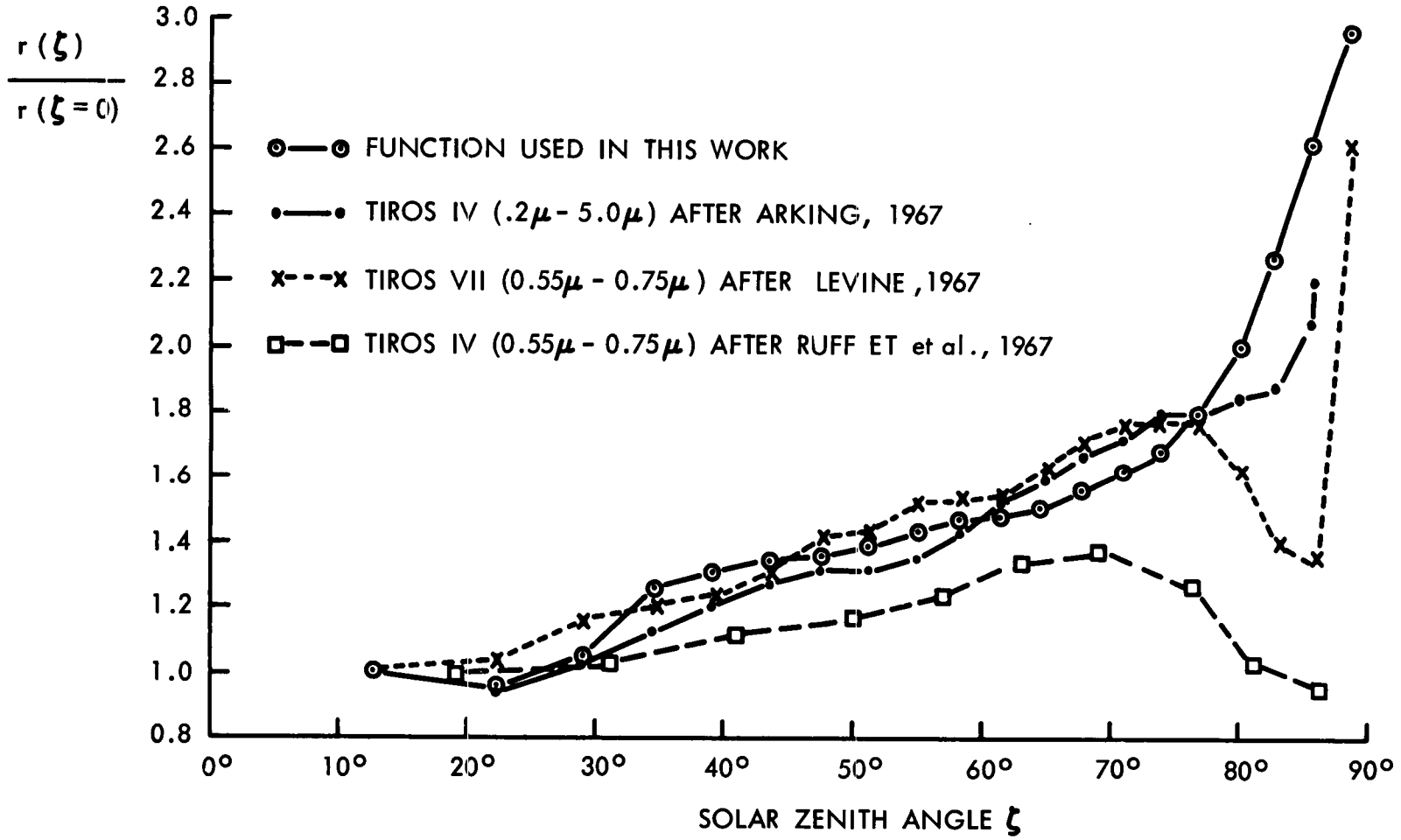

Figure 3. The relative change of the directional reflectance, r, of the earth-atmosphere system with the sun's zenith angle, ζ

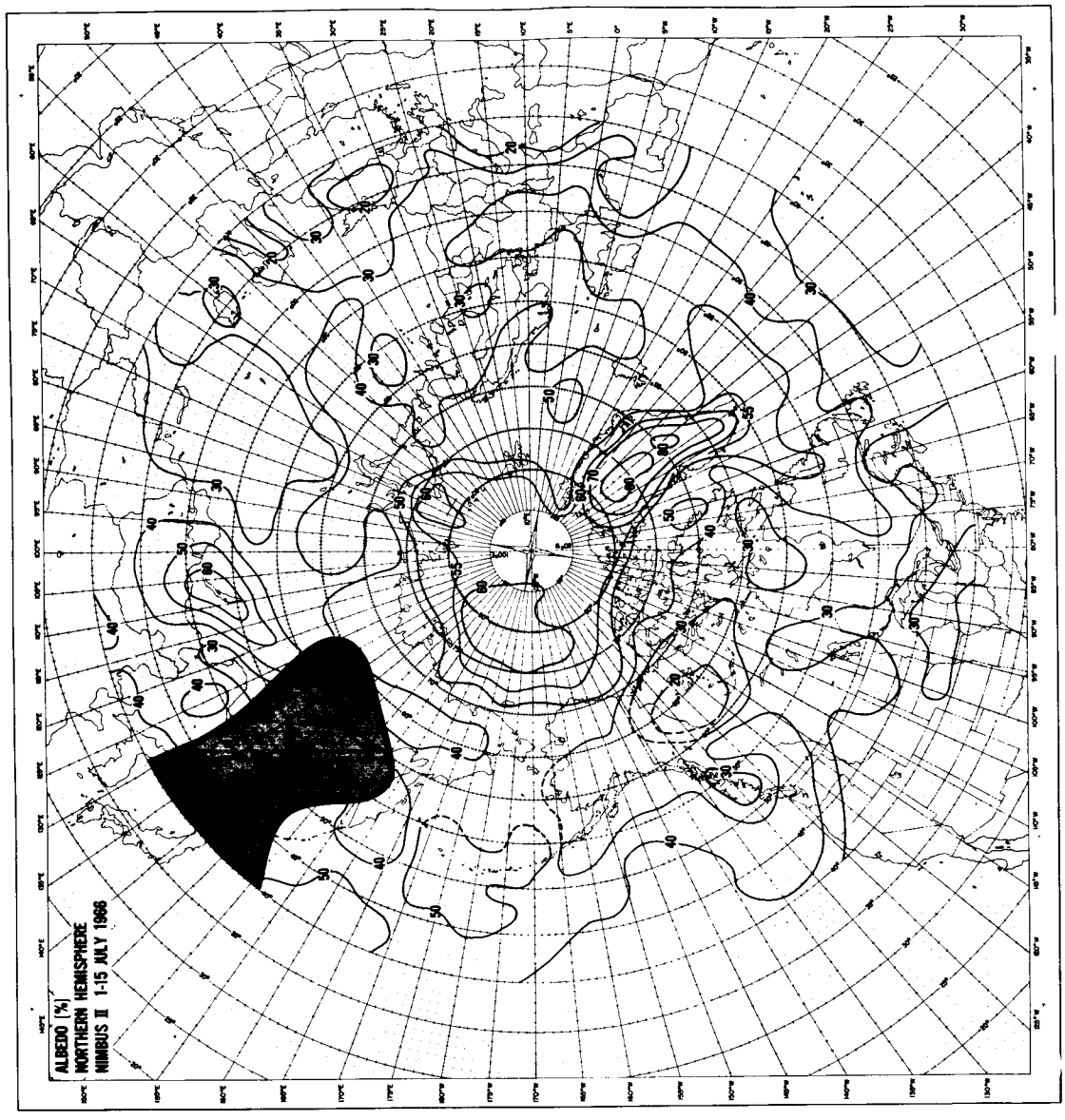

Figure 4. Nimbus II: Albedo [%] of the earth-atmosphere system over the northern hemisphere during the period 1-15 July, 1966

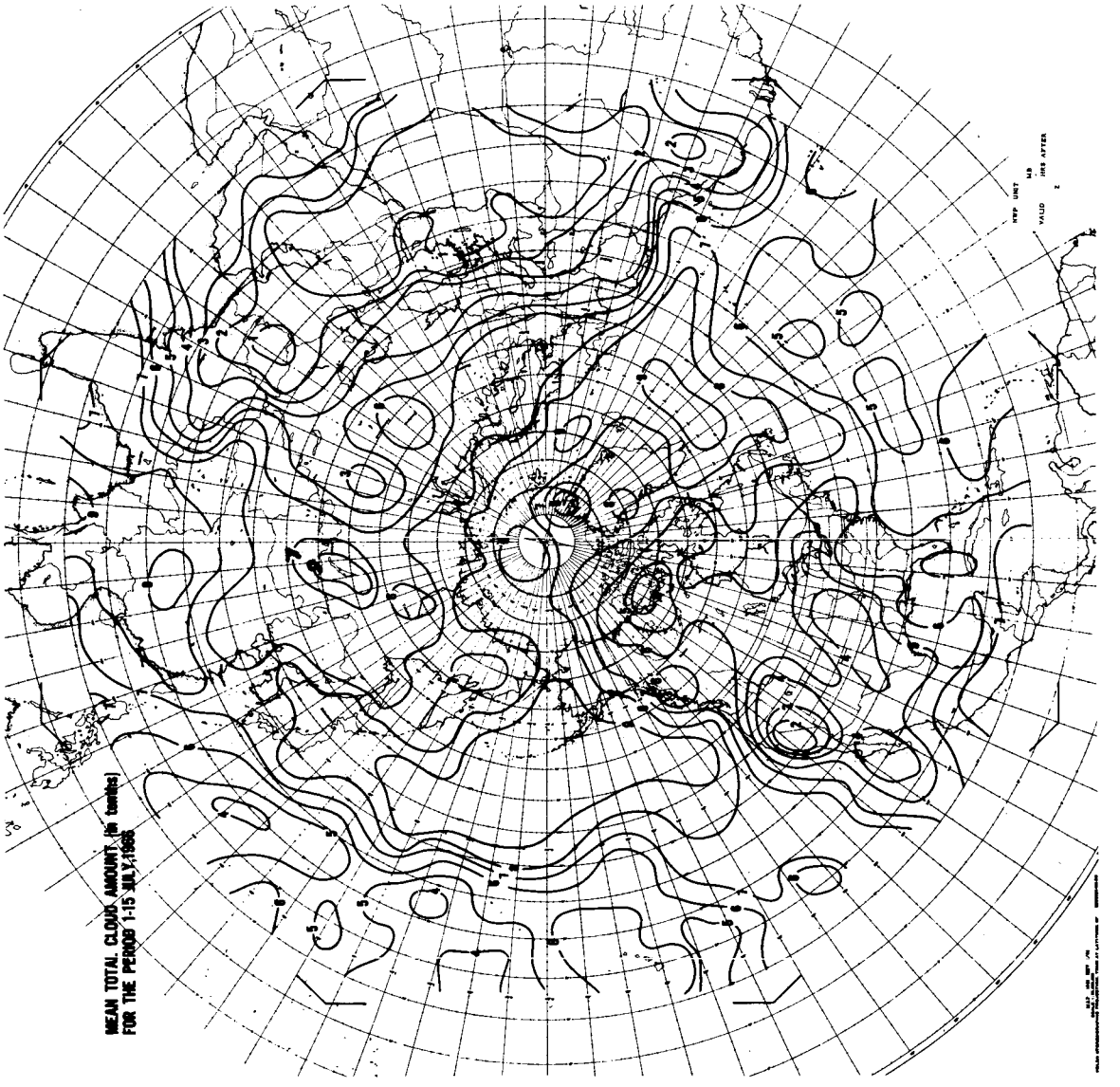

Figure 4a. Mean cloud cover during the period 1-15 July, 1966 from operational data

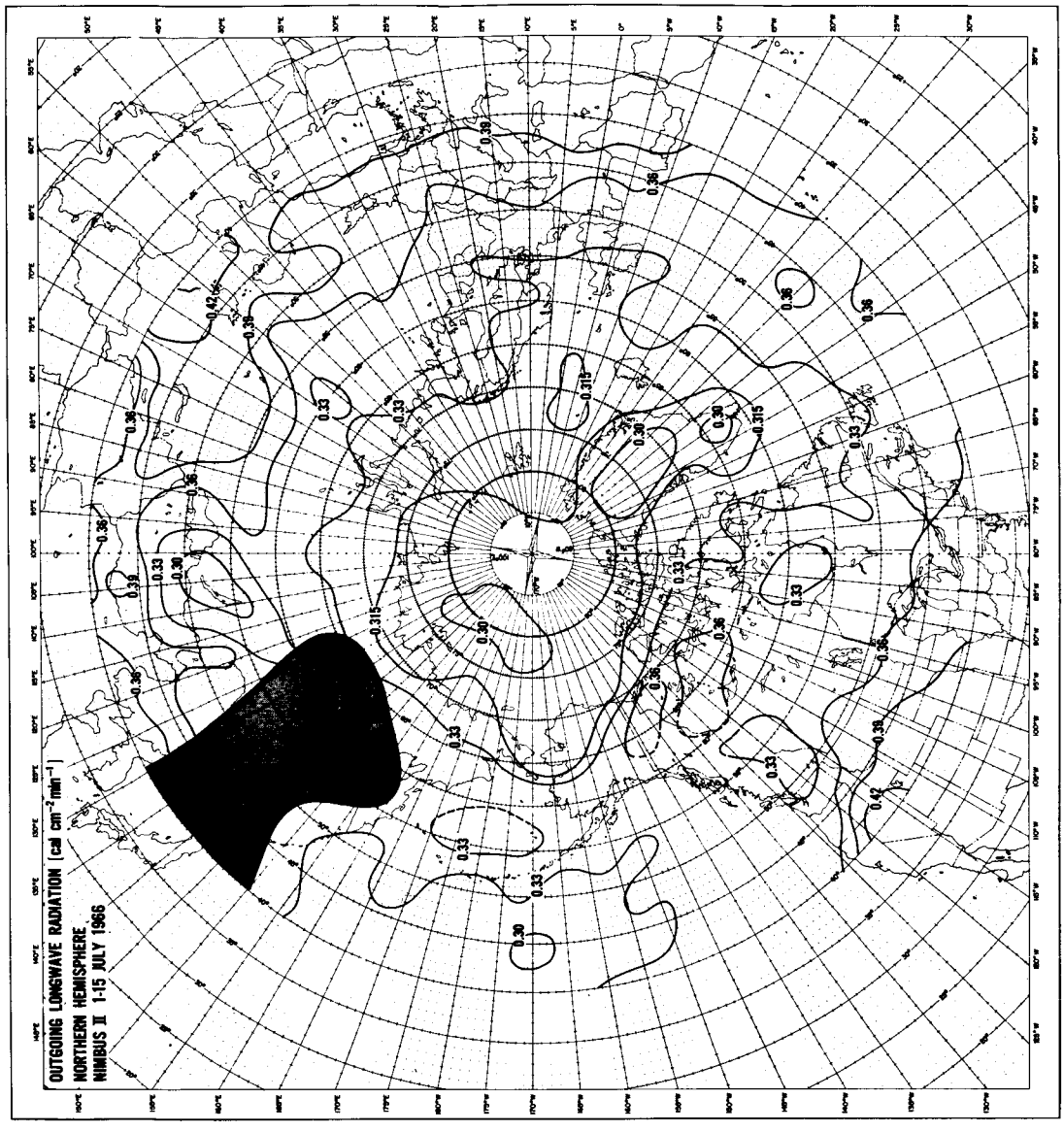

Figure 5. Nimbus II: Total outgoing longwave radiation flux [cal cm^{-2} min^{-1}] over northern hemisphere during the period 1-15 July, 1966

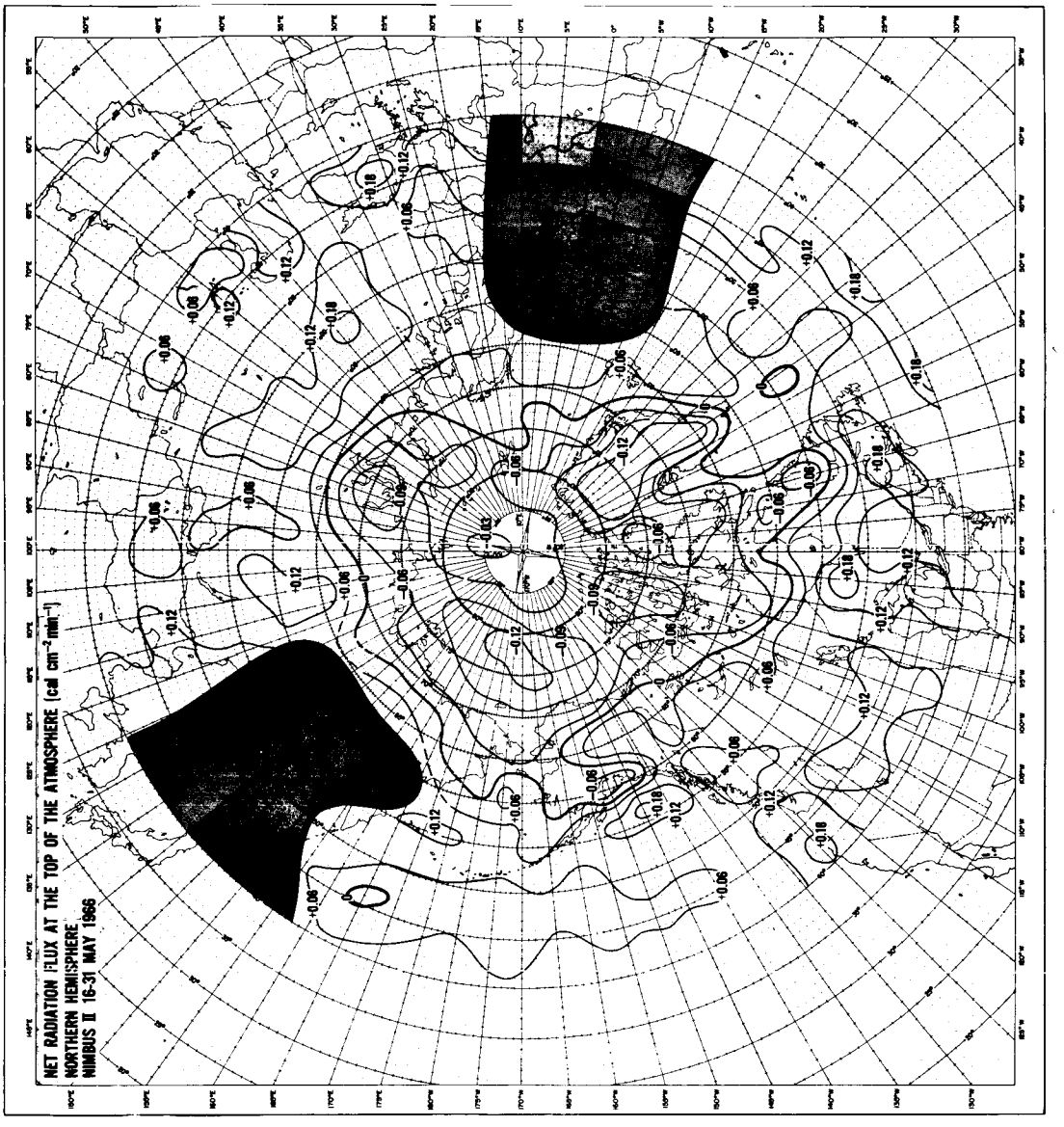

Figure 6. Nimbus II: Radiation balance of the earth-atmosphere system over the hemisphere during the period 16-31 May, 1966

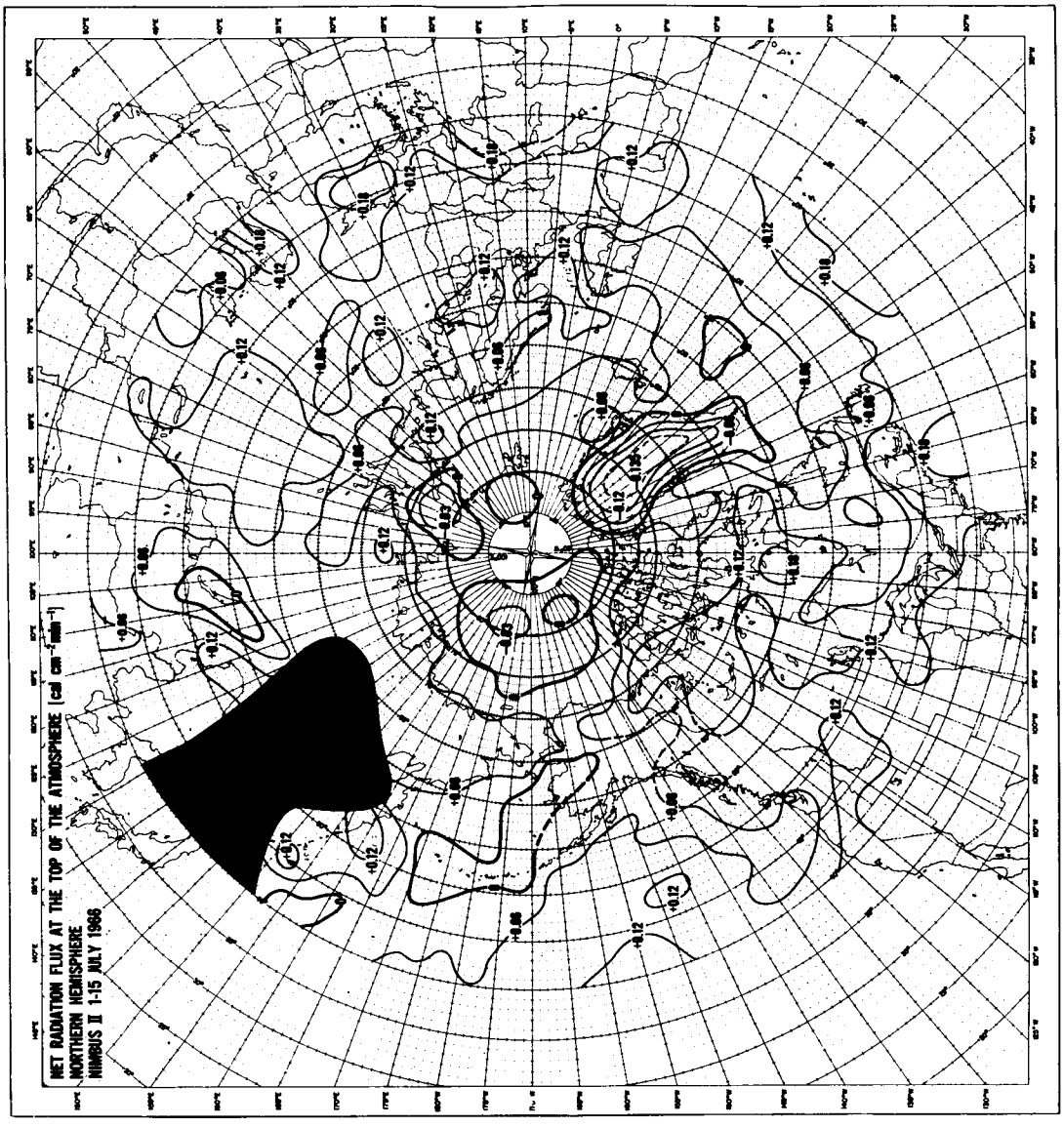

Figure 7. Nimbus II: Radiation balance of the earth-atmosphere system over the hemisphere during the period 1-15 July, 1966

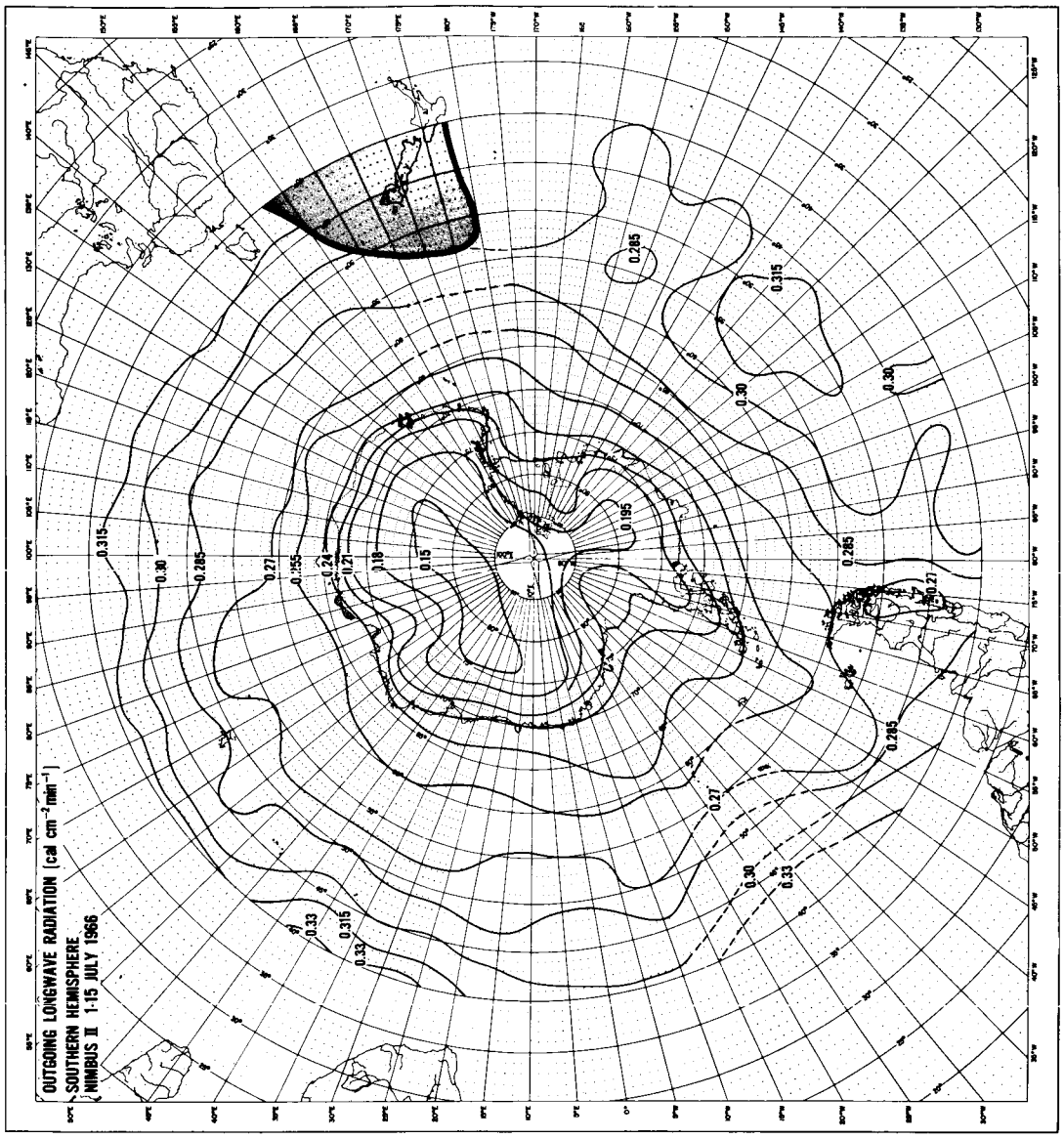

Figure 8. Nimbus II: Total outgoing longwave radiation flux [cal cm^{-2} min^{-1}] over the southern hemisphere during the period 1-15 July, 1966

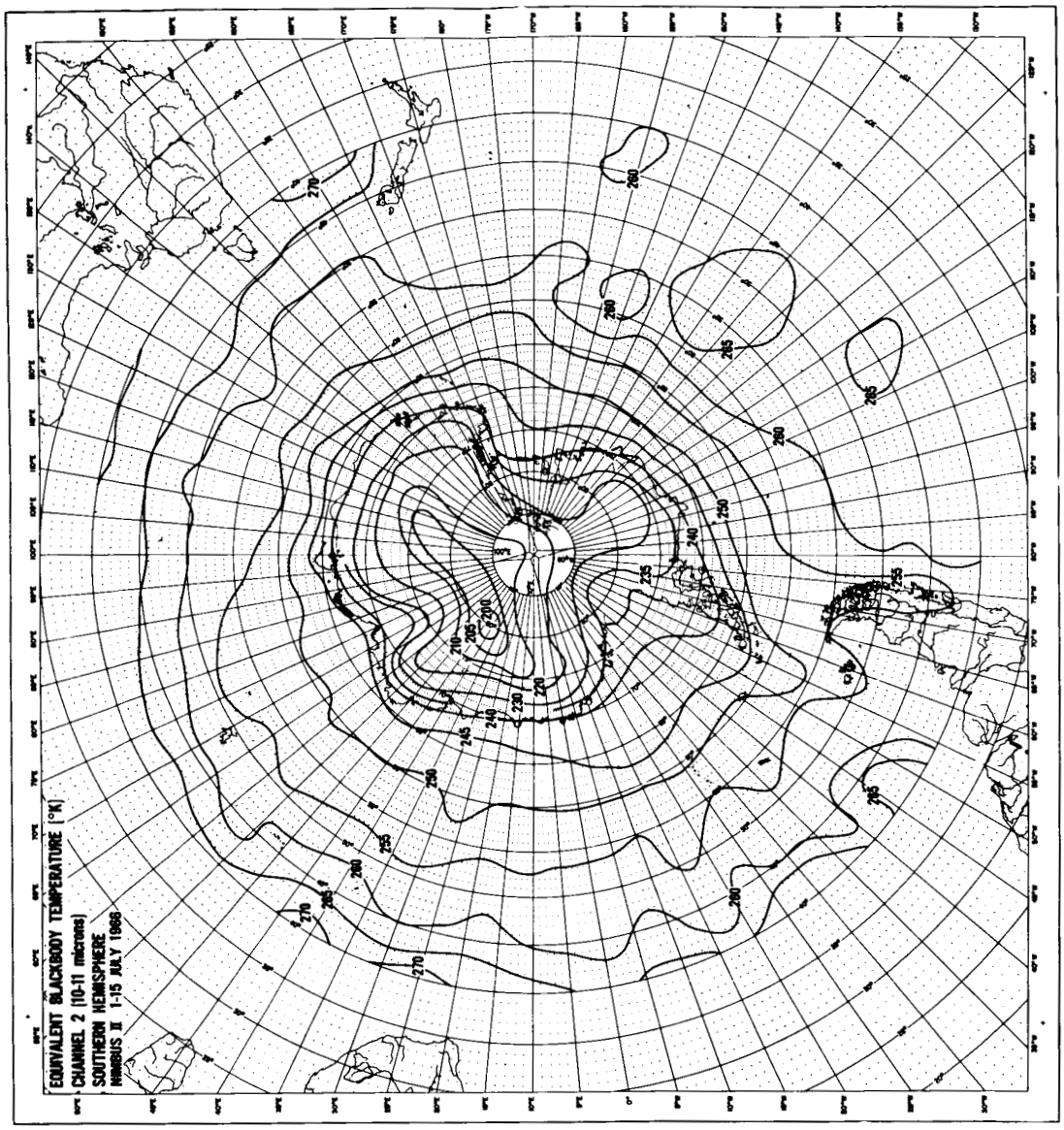

Figure 9. Nimbus II: Equivalent blackbody temperature [°K] of infrared radiation in the spectral range 10-11 microns emerging over the southern hemisphere during the period 1-15 July, 1966

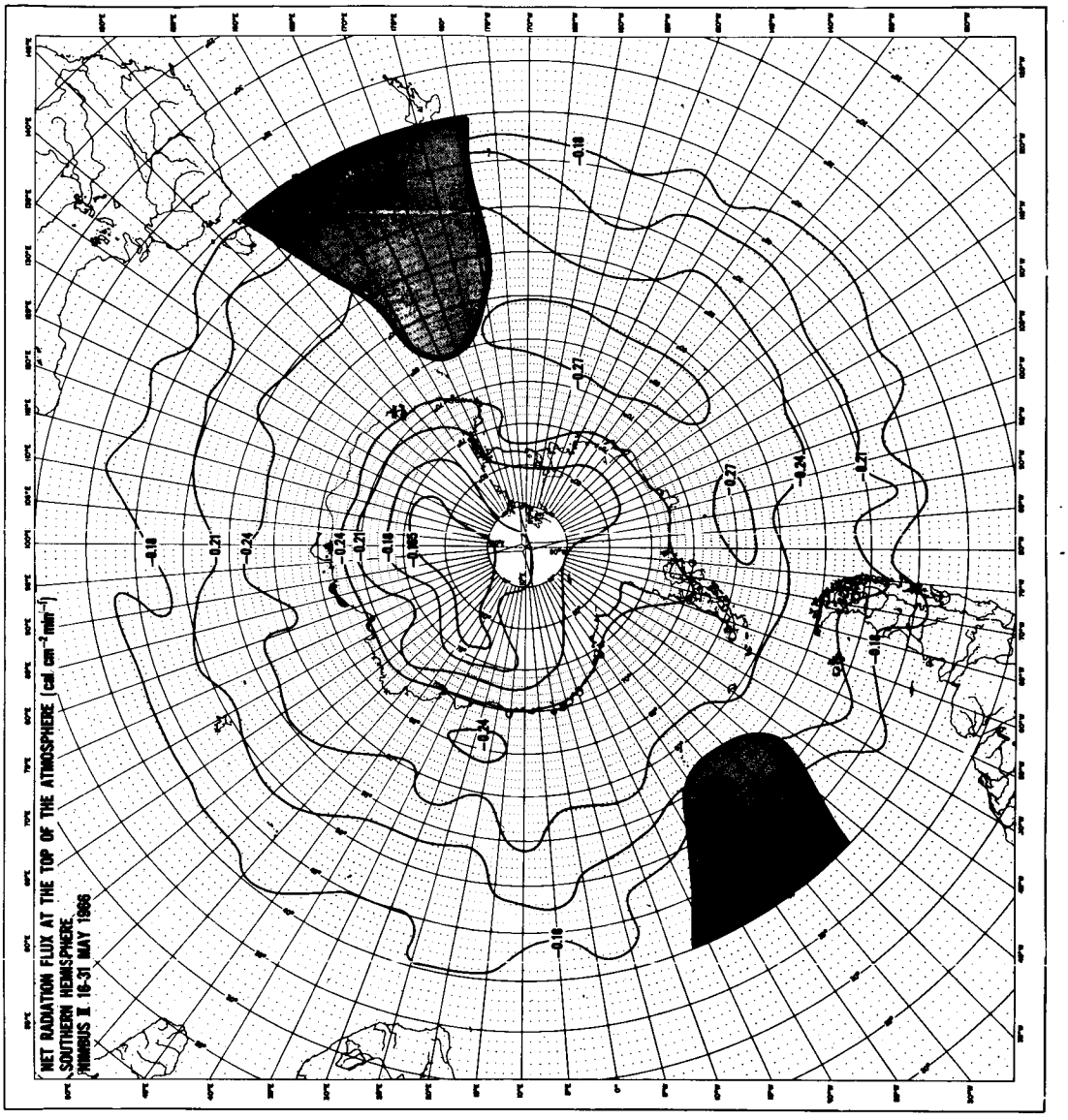

Figure 10. Nimbus II: Radiation balance [cal cm^{-2} min^{-1}] of the earth-atmosphere system over the southern hemisphere during the period 16-31 May, 1966

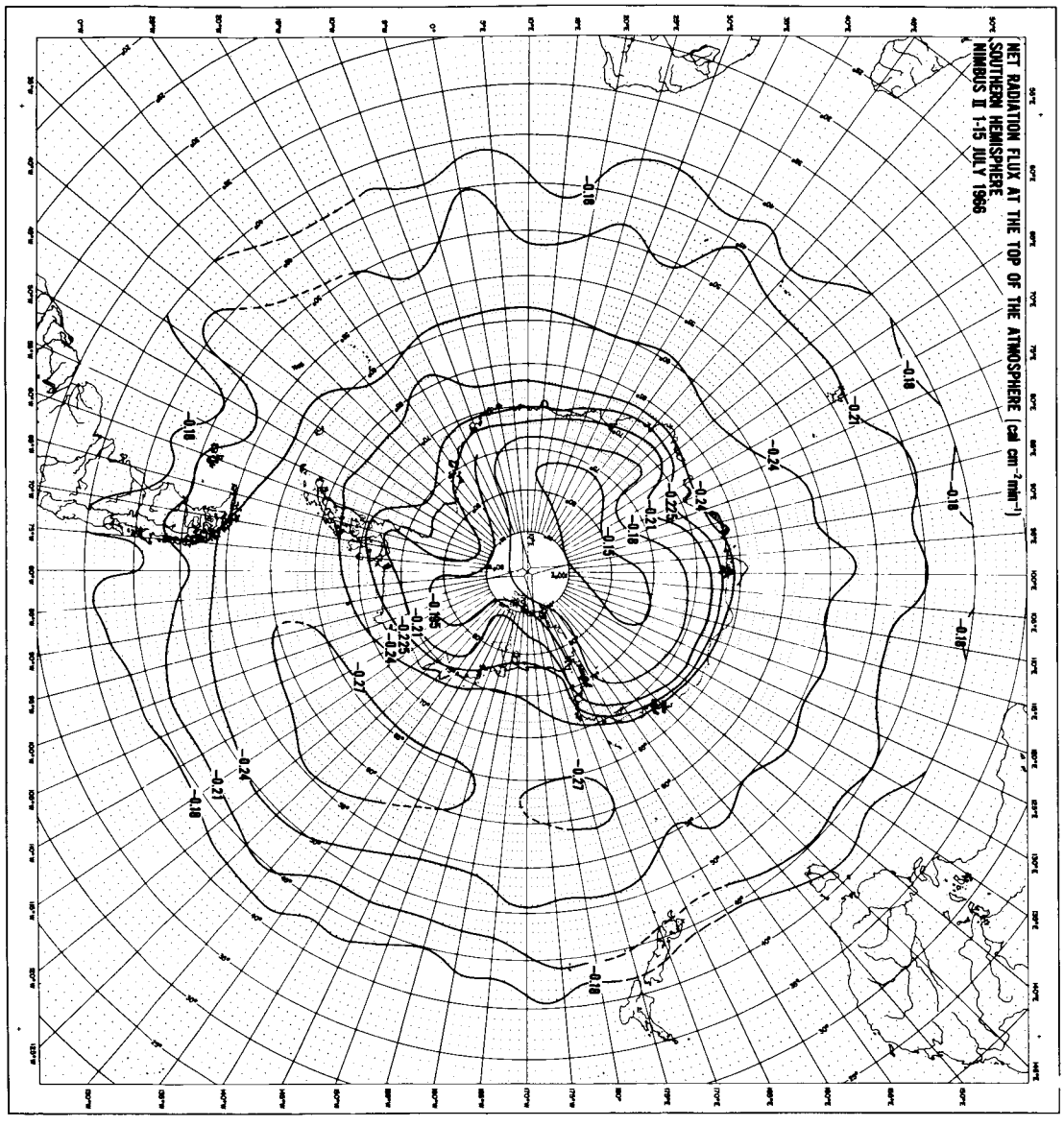

Figure 11. Nimbus II: Radiation balance [cal cm^{-2} min^{-1}] of the earth-atmosphere system over the southern hemisphere during the period 1-15 July, 1966

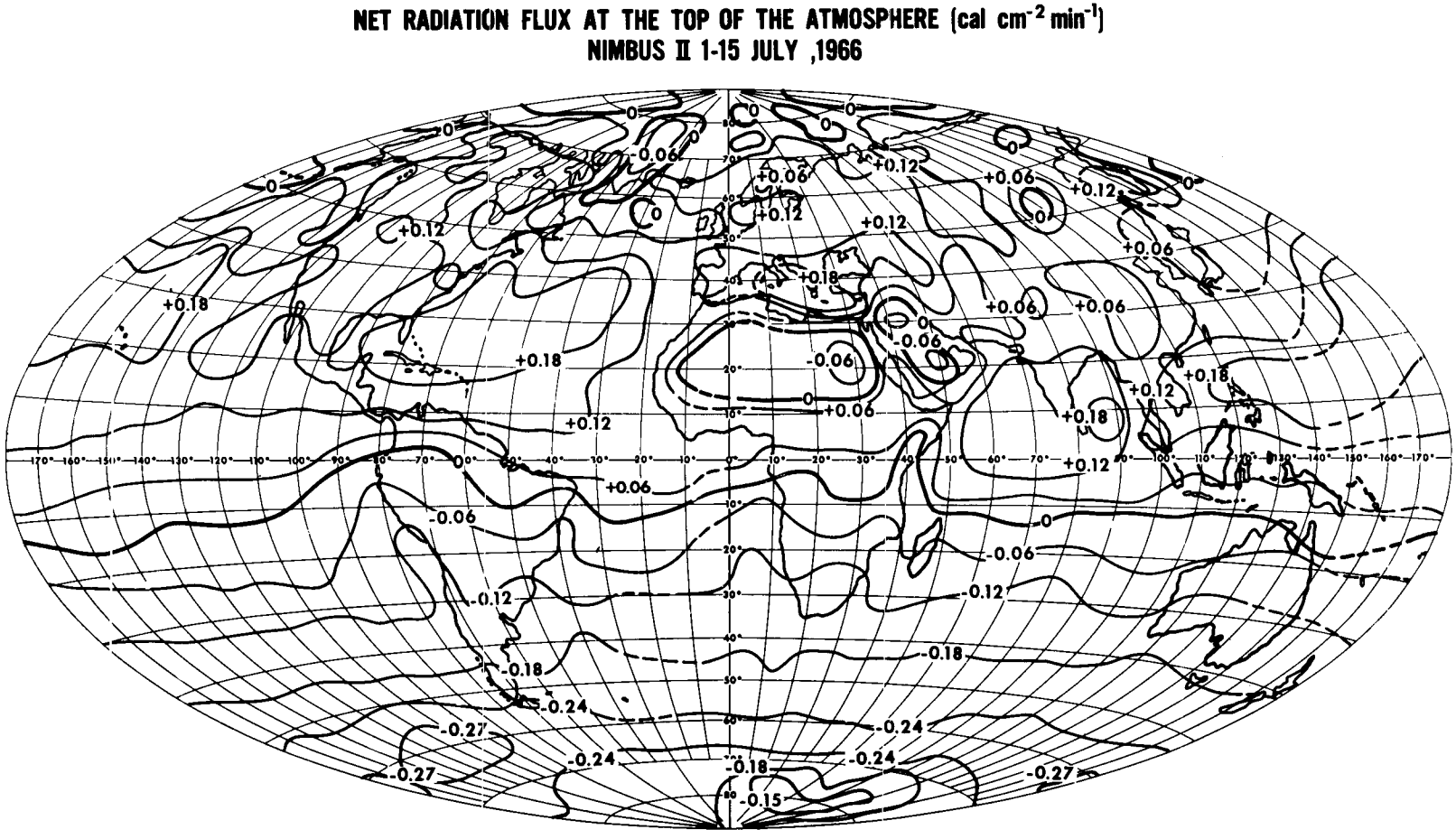

Figure 12. Nimbus II: Radiation balance [cal cm^{-2} min^{-1}] of the earth-atmosphere system over the entire earth during the period 1-15 July, 1966